THE ASTROPHYSICAL JOURNAL 241:981–1000, 1980 November 1

ABUNDANCES IN GLOBULAR CLUSTER RED GIANTS. III. M71, M67, AND NGC 2420

JUDITH G. COHEN
Palomar Observatory, California Institute of Technology; and Kitt Peak National Observatory[1]
Received 1980 March 24; accepted 1980 April 24

ABSTRACT

High-dispersion spectra of four stars in the metal-rich globular cluster M71, four giants in the old open cluster M67, and two members of the metal-poor old open cluster NGC 2420 are analyzed with the aid of model atmospheres. The derived abundances are [Fe/H] = −1.27, −0.39, and −0.61 dex with regard to the Sun for M71, M67, and NGC 2420, respectively. The pattern of elemental abundances is very similar over the full range from M92 to M67, with the most obvious differences being the strong overdepletion of copper, and perhaps scandium, with progressively lower metallicities. The metallicity derived for M71 is much lower than previous estimates, and the consequences of this for the abundance scale of globular clusters and the formation of the halo and disk of the Galaxy are discussed.

Subject headings: clusters: globular — stars: abundances — stars: late-type

I. INTRODUCTION

In this series of papers we attempt to provide fundamental determinations of the abundances of the chemical elements in globular cluster red giants. The first paper of this series (Cohen 1978, hereafter Paper I) described the basic procedure used and presented results for M3 and M13, two globular clusters of intermediate metallicity, while members of the very metal-poor systems M92 and M15 were analyzed in Cohen (1979, hereafter Paper II). In this work we analyze four red giants in M71, believed to be typical of the metal-rich globular clusters, and compare them to red giants in the old open clusters NGC 2420 and M67. The observational material and model atmosphere parameters are described in § II, while the deduced abundances are detailed in § III, where we also discuss the minor improvements in the analysis used here, as compared with Papers I and II. As a result of these minor modifications, we present a correction table to be applied to the abundances of Papers I and II for the five elements affected (V, Cu, Zr, Pr, and Nd). In the next section (§ IV) we compare the deduced abundances in M71, M67, and NGC 2420 with those previously accepted and describe the implications of our suggested revision in the scale of globular cluster abundances for the evolution of the Galaxy. Our study of clusters now spans the full range in metallicity, from M92 and M15 to M71, and the conclusions reached from this long-term effort are summarized in § V. A preliminary account of this work was given by Cohen (1979*b*).

II. OBSERVATIONAL MATERIAL

Four of the bright giants (stars A4, 30, 45, and 46 of Arp and Hartwick 1971) observed in M71 by Frogel, Persson, and Cohen (1979) were selected as program stars. The reddest (and most luminous) M71 giants were not chosen, as they are too cool to yield reliable abundances. Originally, the effective temperatures and surface gravities (with a mass of 0.8 $M_\odot$) derived by Frogel *et. al.*, were used. However, it became apparent that these would yield poor ionization equilibria, and the effective temperatures had to be at least slightly higher. In attempting to match the lunar-occulation temperature scale of Ridgway *et al.* (1980) onto the model atmosphere scale of Cohen, Frogel, and Persson (1978, hereafter CFP) it was apparent that at the cool end of the model atmosphere scale ($3800 \leq T_{\rm eff} \leq 4000$ K) $T_{\rm eff}$ is too low by about 50 K. A small error in the CFP temperature scale could easily arise for such cool, high-metallicity stars as molecules become important opacity sources there. As the reddening in front of M71 is large and somewhat uncertain, an underestimate of the reddening would also reduce the deduced $T_{\rm eff}$ below the true values. A maximum increase in $T_{\rm eff}$ of 100 K can be supported without increasing the reddening beyond a value consistent with the observational data (see the discussion in Frogel, Persson, and Cohen 1979). Most likely a combination of the two problems is occurring, and we have increased $T_{\rm eff}$ by 100 K from the Frogel *et al.* tabulated values and decreased log g 0.1 dex below that corresponding to a mass of 0.8 $M_\odot$. The 0.1 dex uncertainty in surface gravity, depending on which mechanism (reddening, which affects both $T_{\rm eff}$ and luminosity, hence g, or uncertainties in the temperature scale) actually produces most of the temperature change, is not large enough to affect the deduced abundances.

Four members of M67 (stars 105, 170, 224, and 231) were chosen from the group observed by CFP. Because of the high and rapidly increasing line density in high-metallicity stars of cooler $T_{\rm eff}$, two of the coolest giants observed in CFP were combined with two hotter M67 giants to form the sample for that cluster. The very red suspected members in the outer parts of M67 were avoided, since their membership is uncertain, and they are so cool that difficulties in the abundance analysis

[1] Operated by the Association of Universities for Research in Astronomy, Inc., under contract with the National Science Foundation.

TABLE 1

MODEL ATMOSPHERE PARAMETERS

Star	$T_{\rm eff}$	log g	$Z/Z_\odot$	V_t (km s^{-1})
M71:				
30	4050	0.7	1/3	2
45	4050	0.8	1/3	1.5[a]
46	4050	0.8	1/3	2
A4	4100	0.8	1/3	2
M67:				
105	4450	2.2	1	2
170	4300	1.8	1	2
224	4750	2.6	1	1.5[a]
231	4900	3.0	1	2
NGC 2420:				
A	4450	1.7	1/2	1.5[a]
F	4450	1.8	1/2	2

[a] V_t changed to 2 km s^{-1} in final analysis.

would be serious. The $T_{\rm eff}$ and surface gravities tabulated by CFP were adopted with a mass of 1.1 $M_\odot$, although there has been a suggestion (see the note added in proof in CFP) that the reddening of M67 is actually 0.03 mag smaller than the value used by them, which would make the M67 stars 50 K cooler.

Two bright members of the old open cluster NGC 2420 (stars A and F) form the sample for this cluster. The distance modulus, reddening, and visual photometry of McClure, Forrester, and Gibson (1974) were combined with unpublished infrared photometry by Cohen and Persson to determine $T_{\rm eff}$ and surface gravities (assuming a mass of 1.1 $M_\odot$) for the two stars.

As initial guesses, abundances of $\frac{1}{3}$ solar, solar, and $\frac{1}{2}$ solar were chosen for M71, M67, and NGC 2420, based on previous studies of these clusters by other techniques (see § IV). The final adopted model atmosphere parameters for all the giants studied here are listed in Table 1. The proper motion survey of M67 by Murray, Corben, and Allchorn (1965) indicates that three of the sample stars are probably members; the fourth (M67 star 170) is not included in the spatial region covered by the astrometric study. The radial velocities presented in the Appendix to this paper indicate that all the giants in our sample are members of their respective clusters.

As before, all observations were made using the KPNO 4 m echelle spectrograph with the Singer camera, the 79 groove mm^{-1} echelle centered on the blaze, the 226-1 cross disperser centered at 5500 Å, and the H_2 treated or baked IIIa-J emulsion. Two high-quality spectra were taken for each star, except for NGC 2420 star F, where only one good exposure was available. The spectra are listed in Table 2. Sensitometer plates were taken with each exposure and developed simultaneously with the spectra.

The spectra were traced with the PDS digital microphotometer by Mr. Ed Carder of KPNO, converted to intensity, and the lines were identified by using the same procedures and computer software described in Paper I. The basic list of lines measured was that of Paper II, but because of the extremely high line density in these higher-metallicity stars, locating the continuum and avoiding blends became impossible for $\lambda \leq 5180$ Å and equivalent widths were not measured blueward of that. Equivalent widths were determined from all the spectra and weighted as described in Paper I (the weights for each spectrum are listed in Table 2). One plate for each star was measured by the author, the second by one of two research assistants (M. Katz or S. Wilkerson). The weighted W_λ for each star are listed in Table 3. The values of W_λ for lines with a total weight less than 50% of the maximum weight for that star are indicated by a colon. The accuracy of these measurements is similar to those of Papers I and II, for $W_\lambda \leq 50$ mÅ, the error is ± 10 mÅ, while for stronger features the error is $\pm 20\%$.

TABLE 2

PLATE JOURNAL

	Spectrum 1			Spectrum 2		
Star	Number[a]	t (minutes)	Weight	Number[a]	t (minutes)	Weight
M71:						
30	1162	113	4	1166	109	3
45	1233	118	5	1240	165	5
46	1226	96	4	1230	121	3
A4	1170	80	5	1173	140	5
M67:						
105	2023	10	3	2024	10	3
170	2021	10	5	2022	10	5
224	2019	22	4	2020	22	4
231	2017	41	4	2018	41	3
NGC 2420:						
A	2015	47	5	2016	50	5
F	2014	56	3	...	...	...

[a] All spectra are in the SI series (Singer image tube; 4 m echelle).

TABLE 3

MEASURED EQUIVALENT WIDTHS

	Line	EP	log gf	V_t (hfs)	log C_6	M71				M67				NGC 2420	
						30	45	46	A4	105	170	224	231	A	F
LiI	6707.8	0.00	+0.02						43:	≤39	23:	≤34		≤29	
OI	6363.8	0.02	-10.30			22	21	52	23	40	18	18:	12	22:	
NaI	6160.7	2.10	- 1.27				104	52			107:			127	
	6154.2	2.10	- 1.57					40:							
	5895.9	0.00	- 0.19		-30.9					1047	1071	992	771	749	655
	5889.9	0.00	+ 0.11		-30.9					1223	1427	1292	996	1015	865
MgI	5711.1	4.34	- 1.58			114	101	103	103	84	106	115	118	120	97
SiI	6237.3	5.61	- 1.12			56	57	61	29	72	78	113	77	54	66
CaI	6717.7	2.71	- 0.80		-29.7					173	132	149	179	176	147
	6572.8	0.00	- 4.31		-31.2	239	244	226	199	187	214	144	123	213	145
	6166.4	2.54	- 1.30		-29.7	126:	107	98	86	87:	103	106	113:	107	61
	6162.2	1.90	- 0.25		-30.0		265	234			276:			261	
	6161.3	2.52	- 1.31		-29.7		127	105			147:			79	
	5857.5	2.93	+ 0.17		-30.7	185	200	184	163	166	198	190	188	220	177
	5601.3	2.53	- 0.69		-30.4	151	154	163	127	202	234	219	175	206	165
	5590.1	2.52	- 0.66		-30.4	105	117	158:	111	163	172	148	132	118	102
	5588.8	2.53	+ 0.14		-30.4	175	186	209	143	198	224	187	178	194	174
	5582.0	2.52	- 0.54		-30.4	138	136	138	132	145	142	146	126	148	157
ScI	6210.7	0.00	- 1.47	4.9		145	149	188	151	140	168	74	48	96	69
	5724.1	1.43	- 0.77			51	32	75:	31		44	26		36	22
	5717.3	1.44	- 0.66			56	49	51	34:	32	40	36	69		8

TABLE 3—*Continued*

	Line	EP	log gf	V_t (hfs)	log C_6	M71 30	M71 45	M71 46	M71 A4	M67 105	M67 170	M67 224	M67 231	NGC 2420 A	NGC 2420 F
ScII															
	6604.6	1.36	-1.33			71	84	87	65	42	78	88	40	56	71
	6245.6	1.51	-1.27			52	68	67	54	81	91	112	86	73	52
	5239.8	1.45	-0.78			123	131	137	108	130	142	98	82	133	80
TiI															
	6743.1	0.90	-1.31			152	189	176	110	118	158	94	95	138	120
	6556.1	1.46	-0.85			161	164	151	108	124	149	91	121	113	114
	6554.1	1.44	-0.90			126	151	125	78	111	119	60	77	113	76
	6419.1	2.17	-1.12			27	34	44:	13	50	53:	24:	39	42	27
	6359.9	0.05	-3.40			89	79	109	88	76	71	35	17	35	24
	6336.1	1.44	-1.07			45:	97	94	96	91:	64:	62:	21:	57	
	6064.6	1.05	-1.50			125	126	135	107	101	114	65	43	106	90
	6031.7	0.05	-3.37			80	87	82	71	50	72	28	11	48	29
	5922.1	1.05	-1.06			142	105	124	117	142	146	130	82	143	149
	5903.3	1.07	-1.58							100	87	64	34	68	61
	5899.3	1.05	-0.83			180	212	239	171	174	210	156	120	164	153
	5866.5	1.07	-0.52			198	209	186	164	137	174	132	118	174	187
	5774.0	3.30	+0.82			36	62	52	39	58	68	64	42	50	
	5740.0	2.24	-0.34			70	54	59	63	58		53	46	83	32
	5739.4	2.25	-0.31			81	64	61	66	69		42	38	74	53
	5716.5	2.30	-0.09			75	57	50	55	30	47	35	37	30	40
	5490.2	1.46	-0.60			128	120	129	121	102	132	118	71	127	93
	5453.6	1.44	-1.33			62	102	106	101	76	82	63	42	54	59
	5440.5	1.43	-1.65			43	58	43	41	37	26	29		36	14
	5426.3	0.02	-2.60				156	134			80			64	
	5366.7	0.82	-2.15			95	107	119	74	74	101	70	32	69	43
	5338.3	0.83	-1.36			76	109	112	75	78	85	46	32	63	33
	5300.0	1.05	-0.90				81	72						53	
	5295.8	1.07	-1.26					48:							
	5231.0	2.24	-0.60		-31.0	16	25	26	18	51	42	44	10:	14:	
	5219.7	0.02	-1.86			163	192	212	154	132	164	98	97	144	131
	5201.1	2.09	-0.21			85		89:	113	37	66	57	14	66	47
	5192.9	0.02	-0.73			251	276	240	284	172		146	70	170	127

TABLE 3—*Continued*

	Line	EP	log gf	V_t (hfs)	log C_6	M71 30	M71 45	M71 46	M71 A4	M67 105	M67 170	M67 224	M67 231	NGC 2420 A	NGC 2420 F
TiII															
	6559.6	2.05	-2.14			50	50	43	36	80	72	68	66	84	71
	5492.9	1.57	-2.63			53	58	46	39	57	68	64	78:	27	74
	5381.0	1.57	-1.58			180	155	144:	139	125:	154	133	92	160	91
	5336.8	1.58	-1.26			124	127	129	98	98	118	102	86	144	100
	5185.9	1.89	-1.19			221:	121	90	131	74	54:	65:	37	68	58
VI															
	6766.5	1.06	-1.56	2.0		121	115	113	110	72	65	50	23	46	39
	6605.9	1.35	-1.48	2.0		77	121	109	58	80	64	71	28	62	24
	6531.4	1.22	-1.09	2.0		113	116	133	100	90	95	52	62	54	56
	6357.3	1.85	-0.81	2.0		52	29	36:	25		30	24	27	27	19
	6251.8	0.29	-1.59	2.0		130	156	160:	157	105	160	112	83	130	69
	6224.5	0.29	-1.93	2.0		130	151	137	145	139	154	104	81	108	107
	6216.4	0.28	-1.39	2.0		176	205	191	164	174	215	166	132	161	130
	6199.2	0.29	-1.38	2.0		168	209	198	142	129	228	207	119	174	148
	6081.4	1.05	-0.58	2.0		110	138	141	124	106	172	135	94	122	112
	6039.7	1.06	-0.59	2.0		102	116	120	117	119	128	106	78	106	59
	5743.4	1.08	-1.14	2.0		125	151	146	128	127	149	97	59	134	70
	5737.1	1.06	-0.85	2.0		118	130	131	123	116	146	126	68	115	85
	5725.7	2.36	-0.07	2.0		37	32	55:	20	31	72	32	20	31	11
	5703.6	1.05	-0.25	2.0		173:	138	140	120	60:	114	91	75:	104	89
	5632.5	0.07	-3.07	2.0		68	79	61	55	38	57	66	16	47	6:
	5627.7	1.08	-0.57	2.0		114	142	110	118	150	164	132	116	144	109
	5626.0	1.04	-1.46	2.0		84	106	103	99	97	118	60	39	100:	55:
	5605.0	1.04	-1.36	2.0		80	85	96	72	69	80	42	39	85	46
	5240.9	2.37	+0.23	2.0		59	54	55	32	39	64:	27	31	9:	23

TABLE 3—*Continued*

	Line	EP	log gf	V_t (hfs)	log C_6	M71 30	M71 45	M71 46	M71 A4	M67 105	M67 170	M67 224	M67 231	NGC 2420 A	NGC 2420 F
CrI															
	6362.9	0.94	-2.66			104	128	98	80	158	132	121	102	122	74
	6330.1	0.94	-2.76				120	126			80:			108	
	5783.9	3.32	-0.18			29:	60	68:	50	61	58	76	118	94	46
	5746.4	3.85	-0.88			26:	20:	19:	23:	45	22	27	19	11:	10:
	5348.3	1.00	-1.26			219	209	227	191	218	254	180	156	192	173
	5345.8	1.00	-0.98			262	270	312	269	274	302	233	194	261	219
	5296.8	0.98	-1.21					161							
CrII															
	5310.7	4.07	-2.06			16	18	25	8:	15	20	37:	7	33	21
	5237.3	4.07	-1.12			86	69	73	63:	80	76	63	60	62	65
MnI															
	6021.8	3.07	+0.16	3.5		105	130	132	123	142	164	130	145	158	141
	6016.6	3.07	+0.00	5.4		116	145	119	130	144	168	147	156	190	141
	6013.5	3.07	-0.15	3.8		155	154	120	127	154	159	125	144	150	114
	5516.8	2.18	-1.44	8.9		133			116					191	135
	5470.6	2.16	-1.35	7.6		180	217	205	171	196	230	210	155	202	192
	5457.5	2.16	-2.04	5.4		66	86	81	47	117	138	111	68	92	54
	5420.4	2.14	-1.21	11.5				141:							
	5377.6	3.84	+0.47	3.5		119	107	48	55	120	88	109	93	88	49
FeI															
	6769.7	4.58	-2.54			39:	7	34:	19	50	46	24	20	34	15
	6750.2	2.42	-2.64			137	137	114	110	122	122	104	126	156	183
	6739.5	1.56	-4.87			93	61	75	92	85	108	73	72	68	64
	6733.2	4.64	-1.42			28	10:	41:	19:	36	62	68	56	47	65
	6710.3	1.48	-4.91			88:	103	76	21:	105:	59:	71:		70	83
	6703.6	2.76	-3.09				86	85:						112:	
	6593.8	2.43	-2.31			118	130	118	124	123	160	140	142	178	137
	6592.9	2.73	-1.40			153	139	141	147	163	212	163	172	206	153
	6574.3	0.99	-5.09			140	137	140	115	135	141	108	91	146	112
	6569.2	4.73	-0.39			96	111	124	89	142	136	142	91	130	124
	6551.7	0.99	-5.58			107	91	89	77	88	125	60	69	83	81

TABLE 3—*Continued*

	Line	EP	log gf	V_t (hfs)	log C_6	M71 30	M71 45	M71 46	M71 A4	M67 105	M67 170	M67 224	M67 231	NGC 2420 A	NGC 2420 F
FeI (cont.)															
	6421.4	2.28	-2.50			205	184	172	176	175	228	161	138	192	155
	6420.0	4.73	-0.17			79	94	75	65	122	139	121	116	116	128
	6411.7	3.65	-0.37			104	140	147	104	168	176	172	153	181	203
	6408.0	3.69	-1.20			91	141	151	97	193:		163	165	200	134
	6393.6	2.43	-1.78			211	206	217	197	267	294	231	221	236	232
	6392.5	2.28	-4.17			89	82	82	73	98		72	83	78	65
	6358.7	0.86	-4.09			175	169	201	167	171	192	146	149	200	184
	6355.0	2.84	-2.42			113	121	119	129	144	168	179	145	165	140
	6353.8	0.91	-6.41			50	28	51	64	51	56	40	37	62	65
	6336.8	3.69	-0.45			144:	108	118	96	107:	129	157	71:	140	134
	6335.4	2.20	-2.26				166	163		134:	174	135		183	
	6229.2	2.84	-2.96			92:									
	6219.3	2.20	-2.68			124	148	121	136	176	216	134	125	146	159
	6200.3	2.61	-2.76			93	98	100	74	167	188	150	135	153	149
	6180.2	2.73	-2.92			103	116	117	88	114	130	119	125	167	130
	6165.3	4.14	-1.68			104:	38	39	30	52:	56	49	55:	63	61
	6157.7	4.07	-1.45				85	60:			92				
	6065.5	2.61	-1.58			176	196	202	165	226	252	215	192	214	179
	6056.0	4.73	-0.28			54	33	46	52	120	122	104	84	100	91
	6027.1	4.07	-1.16			58	63	78	60	96	118	88	94	120	130
	6008.6	3.88	-0.81			100:	92	81	82	104	138	132	90	148	112
	5910.0	3.21	-2.64			80	67	63	68	111	130	110	83	121	72
	5905.7	4.65	-0.67			54	73	62	54	85	94	88	78	90	95
	5883.8	3.96	-0.57			53	58	81	66	122	88	115	95	118	100
	5862.3	4.55	-0.15			90	79	73	66	62	94	92	102	114	148
	5859.6	4.55	-0.45			57	62	40	47	91	106	114	99	111	100
	5856.1	4.29	-1.62			35	53	35:	34	44	54	49	37	82	72
	5855.1	4.61	-1.59				30	25:	8:	34	26:	34	18	40	16
	5778.5	2.59	-3.60			73	67	63	48	68	84	81	42	98	70
	5775.1	4.22	-1.28			74	70	69	45	78	109	90	75	85	88
	5741.9	4.26	-1.59			49	44	34	36	69	67	60	67	102	47

TABLE 3—*Continued*

	Line	EP	log gf	V_t (hfs)	log C_6	M71				M67				NGC 2420	
						30	45	46	A4	105	170	224	231	A	F
FeI (cont.)															
	5738.2	4.22	-2.14			14:	28	21	8:	50	48	56	40	50	48
	5634.0	4.99	-0.09		-33.9	83	72	46	57	83:	88	99	81	81	93
	5611.4	3.63	-2.93			18	17	32:	12	68	63	59	40	40	55
	5586.8	3.37	-0.42		-30.6	161	180	180	137	211	266	262	219	228	207
	5576.1	3.43	-0.73			176	144	115	135	144	143	152	138		
	5569.6	3.42	-0.69		-30.6	109	110	105	123	130	152	153	146	212	187
	5501.5	0.96	-3.17			242	212	250	195	252	268	227	208	233	194
	5491.8	4.19	-2.23			8	20	30	24	59	50	46	41	56	36:
	5445.0	4.39	-0.34			133	111	107	94	124	121	168	134	158	111
	5441.4	4.31	-1.60			65	51	42	26	53	52	78	56	86	40
	5434.5	1.01	-2.36			313:	334	259	289	299	279:	304	198	258	242
	5373.7	4.47	-0.77			65	56	61	47	86	84	112	74	84	66
	5367.5	4.41	-0.02		-29.9	87	108	116	73	140	148	176	154	122	130
	5322.0	2.28	-2.91			104	111	110	98	82	126	116	95	133	108
	5315.1	4.37	-1.39			73	57	58	54	53	60	71	70	70	67
	5307.4	1.61	-2.99				296	149:	236	156	103	142	100	127	99
	5242.5	3.63	-1.13			68	76	97	75	136	136	111	103	122	104
	5232.9	2.94	-0.25		-30.7	269	251	252	236	409	420	340	301	344	307
	5225.5	0.11	-4.94			255	194	227	233	222:	280	145	74	136	136
	5217.4	3.21	-1.09			83	94	103	80	143	150	132	129	152	123
	5216.3	1.61	-2.57			227	226	234	193	256	275	238	202	269	221
	5198.7	2.22	-2.37			203	170	173	162	112	163	138	100	166	125
	5191.5	3.04	-1.00			164	152	146	242	255:	161	221	167	220	184
FeII															
	6247.5	3.89	-2.53			43	24	19	21	23:	29	70	55	42	47
	6238.4	3.89	-2.70				52	42	24	62	46	53	41	36	39
	5325.6	3.22	-3.24				19:	19:		32	34	41	29	32	46:
	5234.6	3.22	-2.40			40	57	58	67:	100	90	71	60	78	70
	5197.5	3.23	-2.41				63	84	70	56	56	84	54	74	88

TABLE 3—*Continued*

	Line	EP	log gf	V_t (hfs)	log C_6	M71 30	M71 45	M71 46	M71 A4	M67 105	M67 170	M67 224	M67 231	NGC 2420 A	NGC 2420 F
CoI															
	6771.0	1.88	-1.58	10.0		113	150	121	135	150	170	147	130	128	115
	5915.6	2.14	-1.39			51	56	63	35	46	77	52	30	63	48
	5590.8	2.04	-1.33	7.6		54	78	69	51	99	128	92	65	76	68
NiI															
	6772.3	3.66	-0.58			70	52	66	38	67	91	108	82	74	58
	6767.7	1.83	-1.80			133	135	134	130	152	156	116	123	152	131
	6586.3	1.95	-2.58			75	115	90	72	112	129	100	71	118	93
	6532.9	1.93	-2.99			102	106	87	89	58	72	83	76	92	86
	6327.6	1.68	-2.82				92	100:							
	5892.8	1.99	-1.86			113	171	168	140	220	200	206	215	190	168
	5847.0	1.68	-3.17				76	56		60:	65:	68:		70	
	5593.8	3.90	-0.46			20	24	31	20	55	58	50	61	49	37
	5435.9	1.99	-2.24			55:	94	70	58	82	74	56	54	96	54
CuI															
	5782.1	1.64	-1.78	2.0		154	137	111	151	177:	186	188	144	164	147
YI	6222.6	0.00	-1.35				74	53		45	46	18	13:	9:	
ZrI															
	6762.4	0.00	-2.66	2.0		57	78	84	61	60	41	33	42	46	59
	5735.7	0.00	-2.24	2.0		71	83	81	63	36	60	24	11	37	5:
MoI	6030.7	1.53	-0.71	2.0		44	40	46	43	44	53	33:	19	22	8
	5751.4	1.42	-1.10	2.0		10	16	21	35		19	16		12:	20
	5570.4	1.33	-0.56	2.0		50	55	45	63	48	28	47:	26	40:	

TABLE 3—*Continued*

	Line	EP	log gf	V_t (hfs)	log C_6	M71				M67				NGC 2420	
						30	45	46	A4	105	170	224	231	A	F
BaII	5853.7	0.60	-1.00			127:	123	104	106	88	132	86	78	138	144
LaII	6774.3	0.13	-2.82	2.0		47	47	83	42	29:	28	22	47	49	46
	6390.5	0.32	-2.41	2.0		55	50	71	59	64	72	24	21	74	59
PrII	5322.8	0.48	-1.19	2.0		43	52	40	36	16:	18	15	9	38	29:
NdII	5740.9	1.16	-1.27	2.0			41	45							
	5451.1	1.00	-0.70	2.0		119	79	105	83	44	54	24	51	48	66
	5319.8	0.55	-0.96	2.0		87	110	92	81	73	109	102	52	104	135

III. DEDUCED ABUNDANCES

a) Modifications to the Procedures of Paper I

The grid of model atmospheres of CFP has been used with the atomic line parameters of Papers I and II to analyze the line spectrum of the M71, M67, and NGC 2420 giants using the procedure detailed in Paper I. The absorption lines in these high-metallicity stars are in the mean stronger than those of the globular cluster giants previously studied, so that very few lines are actually on the linear part of the curve of growth. Thus the deduced abundances are increasingly sensitive to the adopted damping constants and the microturbulent velocity (V_t). In an effort to minimize this problem, all Fe I and Ti I lines stronger than 150 mÅ were not used in the analysis (although included in Table 3), and the strongest Ni I line was also discarded if larger than this limit. Unfortunately most ions do not have enough weak lines measured to apply this criterion uniformly, but at least some of the remaining worst offenders (particularly Ca I) have individually determined damping constants.

The microturbulent velocity for each star was derived as described in Paper I from lines of Fe I and Ti I and the values are listed in the last column of Table 2. The deduced microturbulent velocities were 2 km s^{-1} for seven of the 10 giants and 1.5 km s^{-1} for the remainder. An error table for changes in abundances produced by small changes in the model atmosphere parameters was constructed for the M71 stars and is given in Table 4. (A slightly modified version of Table 4 was used for the somewhat hotter giants in M67 and NGC 2420.) The largest entry in the error tables for many ions without hyperfine structure corrections was that due to 1 km s^{-1} changes in V_t, as would be anticipated from the generally strong absorption lines. The preliminary abundances were then interpolated to the $T_{\rm eff}$, log g, and V_t given in Table 2 from the results of the closest models in CFP. It was apparent that significantly better internal agreement among the stars in each cluster could be produced by forcing V_t to be the same in all the stars, and thus V_t was changed from 1.5 km s^{-1} to 2 km s^{-1} for the three discrepant stars. The 0.5 km s^{-1} change in V_t is permissible given the uncertainty in this parameter quoted in Paper I.

In the course of reviewing all the atomic line parameters, it was found that the transition probability scale for Zr I and Pr II had not been normalized correctly and that the abundances given in Papers I and II are too high by the constants 0.6 and 0.43 dex, respectively. Furthermore, after careful consideration, the line 5603.8 Å (supposedly Nd II) was deleted from the list of accepted lines; so a small change must be made to the previously published Nd II values. The microturbulent velocity deduced from the many V I lines was consistently too large, implying that a hyperfine structure correction was required. A 2 km s^{-1} hyperfine velocity was introduced in the manner described in Paper I for all V I lines and also for the 5782 Å Cu I line. (The 5105 Å Cu I line used in addition to this line in Papers I and II already had such a correction.) The necessity for including hfs broadening for lines of these particular elements is well documented in the compilation of data by Biehl (1976). This

TABLE 4

SENSITIVITY OF ABUNDANCES TO MODEL PARAMETERS FOR M71 STARS

	CHANGES IN ABUNDANCE (Δ log N/H)				
Ion	$\Delta T_{\rm eff} = +100$ K	$\Delta \log g = +0.5$	$\Delta V_t = +1$ (km s^{-1})	$\Delta V_t = -1$ (km s^{-1})	$\Delta \log Z/Z_\odot = -1.0$
Li I	+0.16	+0.05	−0.02	+0.02	+0.22
O I	+0.04	+0.20	−0.02	+0.02	−0.37
Mg I	−0.03	+0.12	−0.24	+0.38	−0.12
Si I	−0.13	+0.18	−0.06	+0.22	−0.27
Ca I	+0.13	−0.03	−0.47	+0.71	+0.04
Sc I	+0.17	+0.01	−0.03	+0.09	+0.01
Sc II	−0.02	+0.22	−0.16	+0.32	−0.34
Ti I	+0.15	+0.02	−0.17	+0.34	+0.03
Ti II	−0.05	+0.23	−0.24	+0.28	−0.36
V I	+0.15	+0.05	−0.10	+0.13	+0.03
Cr I	+0.11	+0.04	−0.23	+0.22	+0.01
Cr II	−0.13	+0.25	−0.12	+0.26	−0.35
Mn I	+0.03	+0.12	−0.02	+0.01	−0.14
Fe I	−0.03	+0.15	−0.19	+0.41	−0.21
Fe II	−0.22	+0.34	−0.17	+0.26	−0.50
Co I	+0.01	+0.17	−0.01	+0.15	−0.27
Ni I	−0.02	+0.17	−0.21	+0.37	−0.27
Cu I	+0.00	+0.17	−0.25	+0.25	−0.22
Zr I	+0.19	+0.05	−0.04	+0.00	0.00
Mo I	+0.09	+0.11	−0.03	+0.01	−0.10
Ba II	+0.03	+0.22	−0.32	+0.60	−0.10
La II	+0.04	+0.20	−0.05	+0.01	−0.28
Pr II	+0.03	+0.21	−0.03	+0.00	−0.37
Nd II	+0.03	+0.20	−0.09	+0.04	−0.35

modification produces additional small changes in the abundances found in Papers I and II.

We summarize the differences between Papers I and II and the present analysis as follows.

i) *Changes in Procedure*

1. Fe I and Ti I lines with $W_\lambda > 150$ mÅ, and of 5892 Å Ni I if $W_\lambda > 150$ mÅ, are eliminated.
2. V_t is forced to agree for all the stars in each cluster.

ii) *Changes in Atomic Line Parameters*

1. The transition probability scale for Zr I and Pr II has been corrected.
2. The line Nd II 5603.8 Å has been eliminated.
3. $V_{hfs} = 2$ km s^{-1} for all V I lines and for 5782 Å of Cu I.

The corrections which should be applied to the deduced abundances of Papers I and II are listed in Table 5. Aside from the constants for renormalizing the transition probabilities scale for Zr I and Pr II, the largest entry is only 0.16 dex.

b) *The Deduced Abundances*

The final abundances obtained via our analysis as described in Paper I and modified above for 10 giants in M71, M67, or NGC 2420 are listed in Tables 6A–6C. As before, averages weighted by the individual weights for each line are given for ions with six or fewer lines where the unweighted average had an rms deviation of more than 0.2 dex. The abundance for an ion with only one line is given in parenthesis and is not used in the cluster averages if the line had a weight less than 50% of the maximum weight for the star. The elemental abundance in a case where lines of two ions of the same element have been observed is weighted by the number of lines of each ion observed in the star; the cluster mean abundances given in the last two columns of Table 6 are averages of $[\log N/N_H]$ [which is $\log N/N_H(*) - \log N/N_H(\odot)$] for the giants in each cluster, irrespective of the slightly different number of lines observed in the spectra of each of the member stars.

The only reliable ionization equilibrium checks on our procedure are from Ti, Fe, and to a lesser extent Sc, as the two Cr II lines are both crowded and blended. For the two stars in NGC 2420, only in two of the six cases is the difference between the elemental abundance deduced from the neutral and singly ionized lines larger than 0.2 dex, and the mean of the absolute value of the 12 differences is only 0.18 dex. In the case of M71, none of the differences is as large as 0.3 dex, and the mean of the absolute value of the 12 differences is only 0.16 dex, while in M67 this mean is 0.18 dex. Thus the ionization equilibria are quite satisfactory, indicating that the model atmosphere and line parameters are reasonable for these stars.

Using the constant V_t scheme adopted here, the range in abundance from star to star within each cluster for the elements with adequate numbers of lines is very small. Considering only the two best elements, the total range for the four stars in M71 is only 0.05 dex for Ti and 0.21 dex for Fe, with three of the four stars having Fe abundances within 0.03 dex of each other. Similar statements can be made for M67 and NGC 2420. The intrinsic dispersion in abundance of the heavy elements within the members of M67 and M71 thus appears to be very small. Because the single observed O I line is weak, the spread in deduced O abundance within M67 and M71 is probably not real.

The mean Fe abundances are −1.27, −0.39, and −0.61 for M71, M67, and NGC 2420, respectively. The abundances of Table 6 and of Papers I and II (when modified by Table 5) should be correct on a relative scale to within 0.2 dex. It is apparent from the error tables (Table 5 of this paper and Table 5 of Paper I) that the magnitude of the expected errors in T_{eff} and surface gravity are not significant for the abundances in Table 6. The uncertainty in V_t of 0.5 km s^{-1} is more serious in the metal-rich stars for some elements, but the scheme of forcing V_t to a fixed value seems to alleviate that problem. Physically, ignoring interior rotation (all these stars are slow rotators at the surface) and magnetic field effects, there is no reason for V_t to vary within a cluster, and, empirically, fixing V_t seems to give the best results. The difference in metallicity from the initial parameters used (Table 1) to the final results of Table 6 is not large enough to require any adjustment, except perhaps for M71 where one could consider lowering the model atmosphere Z from $\frac{1}{3}$ solar to $\frac{1}{10}$ solar and recomputing the abundances. They would then be on the average about 0.1 dex smaller (see Table 4).

TABLE 5
CHANGES IN PREVIOUSLY PUBLISHED ABUNDANCES

Ion	M92–M15[a] Abundance (dex)	M3–M13[b] Abundance (dex)	Remarks
V I	−0.02	−0.12	[c]
Cu I	+0.00	−0.16	[c]
Zr I	−0.60	−0.60	[d]
Pr II	−0.43	−0.43	[d]
Nd II	−0.10	−0.10	[e]

[a] Applies to the mean cluster abundances in Paper II.
[b] Applies to the mean cluster abundances in Paper I.
[c] Arises as a result of inclusion of hyperfine structure.
[d] Arises as a result of correction in f-value scale.
[e] Arises because of eliminating the line at 5603.8 Å.

TABLE 6A

ABUNDANCES FOR M71 GIANTS

ELEMENT	Star 30 abundance	No.of Lines	Star 45 abundance	No of Lines	Star 46 abundance	No. of Lines	Star A4 abundance	No. of Lines	Mean for Cluster	$[N/N_{Fe}]$
LiI							(-1.04)	1	(-1.04)	(+0.23)
OI[a]	-1.12	1	-1.15	1	-0.66	1	-1.10	1	-0.71	+0.56
NaI			-0.58	1	-0.92	1			-0.74	+0.53
MgI	-1.16	1	-1.36	1	-1.32	1	-1.32	1	-1.29	-0.02
SiI	-0.38	1	-0.40	1	-0.32	1	-0.93	1	-0.51	+0.76
CaI	-0.59	7	-0.55	9	-0.53	9	-0.88	7	-0.64	+0.63
ScI	-0.70	3	-0.84	3	-0.65	3	-0.87	3	-0.82	+0.45
-0.81			-0.80		-0.69		-0.98			
ScII	-0.92	3	-0.76	3	-0.74	3	-1.08	3		
TiI	-0.77	19	-0.79	16	-0.74	21	-0.76	29	-0.74	+0.53
-0.71			-0.73		-0.74		-0.76			
TiII	-0.50	5	-0.53	5	-0.77	5	-0.79	5		
VI	-0.87	19	-0.62	19	-0.76	19	-0.94	18	-0.80	+0.47
CrI	-1.42	5	-1.19	6	-1.31	7	-1.40	5	-1.13	+0.14
-1.13			-1.03		-1.10		-1.24			
CrII	-0.40	2	-0.53	2	-0.35	2	-0.85	2		
MnI	-1.36	7	-1.23	6	-1.45	7	-1.50	7	-1.39	-0.12
FeI	-1.21	47	-1.23	49	-1.24	49	-1.44	49	-1.27	0.00
-1.22			-1.21		-1.23		-1.42			
FeII	-1.36	2	-1.00	5	-1.08	5	-1.23	4		
CoI	-1.20	3	-1.18	3	-1.17	3	-1.33	3	-1.22	+0.05
NiI	-1.37	7	-1.30	8	-1.23	8	-1.39	7	-1.32	-0.05
CuI	-1.24	1	-1.41	1	-1.35	1	-1.28	1	-1.45	-0.16
YI			-0.85	1	-1.25	1			-1.05	+0.22
ZrI	-1.00	2	-0.78	2	-0.79	2	-1.25	2	-0.96	+0.31
MoI	-1.31	3	-1.22	3	-1.18	3	-1.02	3	-1.18	+0.09
BaII	-1.14	1	-1.18	1	-1.49	1	-1.45	1	-1.31	-0.04
LaII	-0.50	2	-0.50	2	-0.16	2	-0.49	2	-0.41	+0.86
PrII	-0.47	1	-0.34	1	-0.52	1	-0.56	1	-0.47	+0.80
NdII	-0.51	2	-0.44	3	-0.45	3	-0.81	2	-0.55	+0.72

Notes: a) Mean for cluster includes a 0.3 dex CO correction.

TABLE 6B

ABUNDANCES FOR M67 GIANTS

ELEMENT	Star 105 Abundance		No. of Lines	Star 170 Abundance		No. of Lines	Star 224 Abundance		No. of Lines	Star 231 Abundance		No. of Lines	Mean for Cluster	[N/N_{Fe}]
LiI	≤-0.42		1	(-1.06)		1	≤-0.06		1				(-1.06)	(-0.67)
OI[a]	+0.03		1	-0.58		1	-0.15		1	-0.16		1		
COcorr.	+0.20			+0.30			0			0			-0.09	+0.30
NaI	-0.22		2	-0.32		3	-0.26		2	-0.01		2	-0.20	+0.10
MgI	-1.22		1	-1.07		1	-0.66		1	-0.48		1	-0.85	-0.46
SiI	+0.04		1	+0.13		1	+0.59		1	+0.06		1	+0.21	+0.60
CaI	-0.12		8	-0.15		10	-0.08		8	-0.00		8	-0.09	+0.30
ScI	-0.35	-0.25	2	-0.36	-0.26	3	-0.08	+0.03	3	+0.25	-0.01	2	-0.12	+0.27
ScII	-0.18		3	-0.16		3	+0.14		3	-0.18		3		
TiI	-0.22	-0.20	23	-0.36	-0.28	19	-0.17	-0.13	24	-0.17	-0.17	24	-0.20	+0.19
TiII	-0.09		5	+0.03		5	+0.07		5	-0.18		5		
VI	-0.27		18	-0.44		19	-0.16		19	-0.18		18	-0.26	+0.13
CrI	-0.41	-0.31	5	-0.78	-0.58	6	-0.18	-0.15	5	-0.20	-0.25	5	-0.32	+0.07
CrII	-0.05		2	+0.04		2	-0.06		2	-0.37		2		
MnI	-0.63		6	-0.78		6	-0.41		6	-0.31		6	-0.53	-0.14
FeI	-0.47	-0.45	45	-0.48	-0.48	41	-0.28	-0.28	46	-0.33	-0.35	50	-0.39	0.00
FeII	-0.30		5	-0.49		5	-0.28		5	-0.55		5		
CoI	-0.44		3	-0.42		3	-0.25		3	-0.25		3	-0.34	+0.05
NiI	-0.55		7	-0.60		7	-0.39		7	-0.34		6	-0.47	-0.08
CuI	-0.35		1	-0.41		1	-0.04		1	-0.27		1	-0.27	+0.12
YI	-0.53		1	-0.80		1	-0.60		1	-0.58		1	-0.63	-0.24
ZrI	-0.27		2	-0.58		2	-0.09		2	-0.12		2	-0.27	+0.12
MoI	-0.43		3	-0.85		3	-0.10		3	-0.17		2	-0.39	0.00
BaII	-0.91		1	-0.39		1	-0.79		1	-0.66		1	-0.69	-0.30
LaII	+0.27		2	+0.12		2	+0.13		2	+0.40		2	+0.23	+0.62
PrII	-0.15		1	-0.29		1	+0.04		1	-0.02		1	-0.11	+0.28
NdII	-0.20		2	-0.09		2	+0.21		2	+0.11		2	+0.01	+0.40

Notes

a. Does not include the correction for O tied up in CO listed below.

TABLE 6C

ABUNDANCES FOR NGC 2420 GIANTS

Element	Star A Abundance	No. of Lines	Star F Abundance	No. of Lines	Mean for Cluster[b]	$[N/N_{FE}]$
LiI	≤ -0.58	1			≤ -0.58	≤ +0.03
OI[a]	(-0.59)	1			(-0.29)	(+0.32)
NaI	-0.58	3	-0.49	2	-0.55	+0.06
MgI	-0.86	1	-1.16	1	-0.96	-0.35
SiI	-0.53	1	-0.32	1	-0.46	+0.15
CaI	-0.19	10	-0.42	8	-0.27	+0.34
ScI	-0.40	2	-0.55	3		
-0.48			-0.66		-0.54	+0.07
ScII	-0.54	3	-0.78	3		
TiI	-0.39	24	-0.49	20		
-0.38			-0.50		-0.42	+0.19
TiII	-0.32	5	-0.52	5		
VI	-0.54	19	-0.63	19	-0.57	+0.04
CrI	-0.54	6	-0.95	5		
-0.49			-0.82		-0.60	+0.01
CrII	-0.32	2	-0.41	2		
MnI	-0.75	7	-0.95	7	-0.82	-0.21
FeI	-0.54	40	-0.65	45		
-0.58			-0.66		-0.61	0.00
FeII	-0.88	5	-0.74	5		
CoI	-0.73	3	-0.75	3	-0.73	-0.12
NiI	-0.65	7	-0.92	6	-0.74	-0.13
CuI	-0.68	1	-0.84	1	-0.73	-0.12
YI	(-1.38)	1			(-1.38)	(-0.77)
ZrI	-0.42	2	-0.46	2	-0.43	+0.18
MoI	-0.78	3	-0.81	2	-0.79	-0.18
BaII	-0.48	1	-0.34	1	-0.43	+0.18
LaII	+0.22	2	+0.12	2	+0.19	+0.80
PrII	-0.01	1	-0.10	1	-0.04	+0.57
NdII	-0.24	2	+0.04	2	-0.15	+0.47

Notes: a) Mean for cluster includes 0.3 dex CO correction.
b) Abundances from star A have double weight.

The adopted absolute normalizations for solar metallicity were carefully reviewed, especially for the elements with only a few weak lines (i.e., those with atomic numbers greater than 30, excepting Ba II). Our absolute scale is based for these elements on assuming the validity of the Corliss and Bozman (1962) tabulations to define the relative transition probabilities. With the new normalization for Pr II and Zr I discussed earlier, we evaluate the maximum possible error in the absolute scale as the larger of the standard deviation of the mean for the strongest lines of those elements present in the Sun or the deviation of the particular lines observed in the M71, M67, and NGC 2420 giants from the mean values. The results are summarized in Table 7. The only elements in this class whose abundances could be severely overestimated (by more than 0.3 dex) are Y and Zr. We shall return to this point later.

Another area of uncertainty which has been explored in a preliminary way is the affect of molecules on the atmospheric temperature-depth structure. The ATLAS code (Kurucz 1979) on which our model atmosphere grid is based does not include molecules. Therefore since the usual effect of molecules is to cool the surface and slightly warm the interior (Gustafsson *et al.* 1975), we artifically modified the $T - \tau$ relationship for a CFP model by cooling the outer layers by 50 K, and similarly increasing T in the deeper layers. The resulting change in deduced abundance for an M71 star was less than 0.15 dex for all elements, and less than 0.10 dex for 80% of the elements. It does not appear that our neglect of molecules can be very serious, and it certainly cannot significantly affect the relative abundances within the three clusters studied here.

In Figure 1 we plot the mean cluster abundances $[N/N_{Fe}]$ for the three clusters studied here, for M13 from Paper I, and for M92 from Paper III. The published abundances in M13 and M92 have been corrected according to the precepts of Table 5. Uncertain cases (Co and Si in M92, O and Y in NGC 2420, and Li in M71) have been omitted. Elements of consecutive atomic numbers with determined abundances are connected by lines.

The general resemblance of the abundance pattern from M67 at [Fe/H] = −0.39 to M92 ([Fe/H] = −2.34) is remarkable. The overdepletion of the odd atomic numbers predicted by most theories of explosive nucleosynthesis (e.g., Arnett 1971) is never larger than 0.4 dex for the well-determined group from Ca to Ni, is that large only for Sc and Mn, and is already 0.2 dex in NGC 2420. Thus the predicted rapidly increasing odd-even alteration as Z is decreased is not seen. The largest difference among the clusters appears to be the increasing deficiency of Cu as Z decreases, but since there are at most only two Cu I lines in each star, and the element does require hyperfine structure corrections, the reality of this apparent change in Cu/Fe is debatable. Considering the group La-Ce-Pr-Nd as a whole, there is a marginally believable trend in that the mean ratio of rare earths/Fe decreased from 0.5 dex for M67 and NGC 2420 to 0.35 dex in M13, and finally to 0.0 dex for M92, but there are very few lines that are reliable in the latter case. Given the uncertainties in the rare earth absolute normalizations shown in Table 7, one can only assert that ratio of rare earths/Fe in the M67 and NGC 2420 giants is solar or larger, but not below the solar value. Even the elements slightly beyond the Fe peak do not drop off noticeably more rapidly as the metallicity is decreased over the total range spanned by globular clusters. [O/Fe] appears to behave similarly to [Ca/Fe], and the latter ratio (and the slope through the even iron peak elements between Ca and Fe) seems slightly larger in most globulars, so that compared to open clusters, [O/Fe] may be up to 0.3 dex larger. But the outstanding characteristic of Figure 1 is the similarity of abundance distribution over this wide range $-2.3 \leq [Fe/H] \leq -0.4$, especially for the best-determined elements from atomic numbers 20 to 28. However and wherever these elements were synthesized and ejected into the protostars which became the old giants we see today, the process was to first order identical over large ranges of space and time for these heavy elements.

TABLE 7

MAXIMUM ERRORS IN ABUNDANCES RELATIVE TO THE SUN, WHICH ARISE FROM UNCERTAINTIES IN THE ABSOLUTE SCALE OF THE TRANSITION PROBABILITIES[a]

Ion	Positive	Negative
Y I	+0.4	−0.4
Zr I	+0.2	−0.7
Mo I	+0.2	−0.2
La II	+0.4	−0.2
Ce II	+0.3	−0.2
Pr II	+0.3	−0.3
Nd II	+0.3	−0.3

[a] Maximum error in $[N/H] = \log (N/N_H)_* - \log (N/N_H)_\odot$.

IV. IMPLICATIONS OF THE ABUNDANCE FOUND FOR M71

a) *Comparison with Previous Determinations*

The abundance we have obtained for M71, [Fe/H] = −1.27 dex, is considerably lower than previous estimates for this cluster. Before considering the implications of this result, we review the older determinations to try to understand from whence arose the widespread belief that [Fe/H] = −0.3 dex for M71.

Let us first recall that the reddening for this globular cluster is large and somewhat uncertain, and since $b_{II} = -5°$, there is a severe problem of field star contamination. Arp and Hartwick (1971) used UBV photometry to determine $E(B - V)$ and then $\delta(U - B)$, from which they obtained $[Fe/H]_{M71} = -0.3$. However, their reddening was obtained from force fitting the M71 color-magnitude diagram to that of 47 Tuc, but the 47 Tuc photometry they used (Tifft 1963) contained a then unrealized 0.08 mag error in $B - V$ (see Hartwick and Hesser 1974). This error is sufficiently large enough to have affected $\delta(U - B)$ and hence their abundance determination. Butler's (1975) ΔS analysis also gave a high abundance ($[Fe/H]_{M71} = -0.04$), but it is, as he admits, based on one star, which is not an RR Lyrae variable and

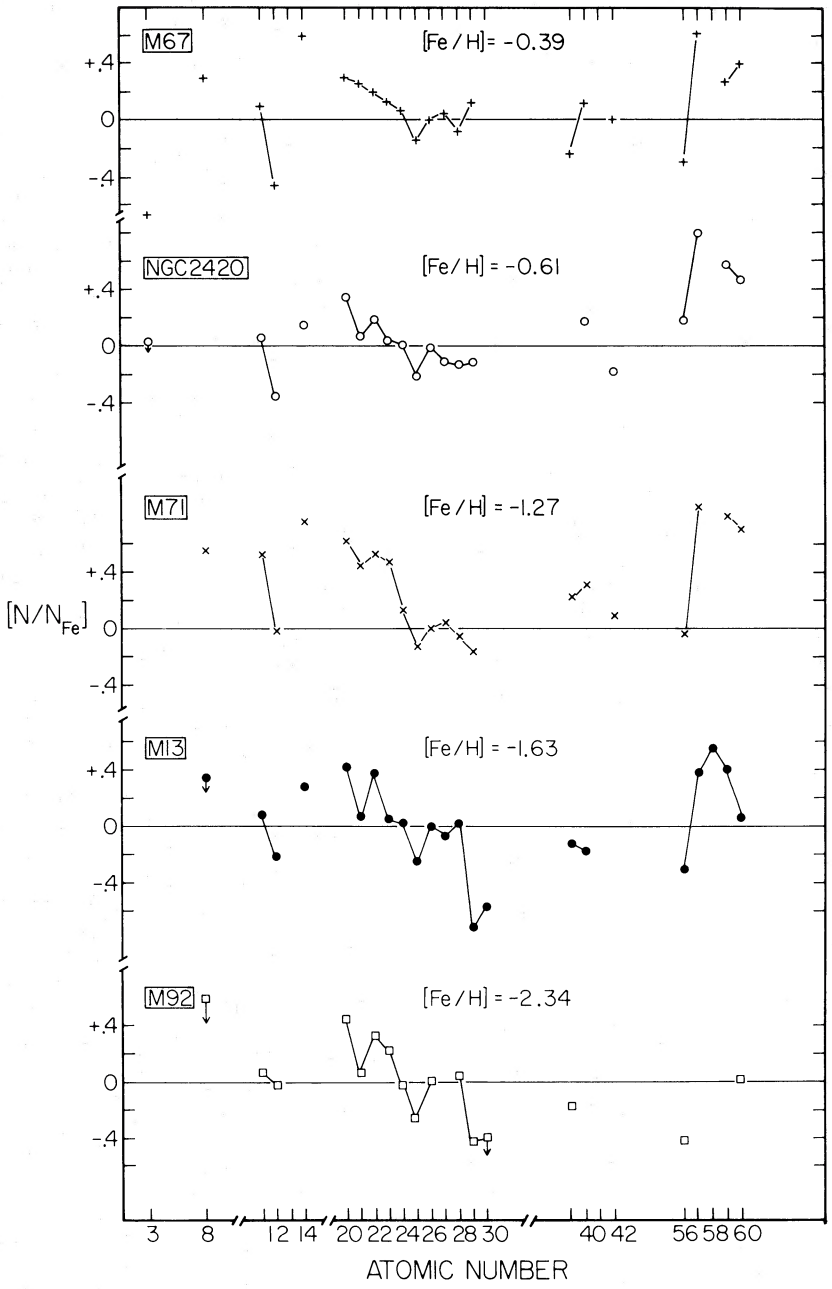

FIG. 1.—The abundances of elements relative to iron are plotted as a function of atomic number for stars in M67, NGC 2420, M71, M13, and M92. The abundances are averaged over the stars in each cluster and are taken from Paper I for M13 and Paper II for M92. The iron abundance is also indicated for each cluster, and when the abundances are determined for consecutive atomic numbers, they are connected by straight lines.

may well not be a cluster member. Canterna's (1975) Washington photometry for six stars (giving $[Fe/H]_{M71} = -0.3$) may also be contaminated by field stars, as the supposed M71 cluster members scatter more widely than those of any other globular in his two color diagram (see Figure 1 of Cantera 1975). Turning to DDO photometry, Hesser, Hartwick, and McClure (1977) adopted solar metallicity for M71, after stating that the calibrations then available for DDO photometry indicated [Fe/H] at least as low as -1.0 dex and ascribing this result to problems in the calibration of DDO photometry for metal-rich globular cluster stars. Mould and McElroy's (1978) value of -0.4 dex from TiO band photometry and Frogel, Persson, and Cohen's (1979) -0.4 dex from CO indices suffered from very uncertain calibrations and from assuming that O/Fe is solar, while $[O/Fe]_{M71} = [Ti/Fe]_{M71} = +0.55$ dex from Table 6. All other tabulations of which I am aware merely combined and weighted these determinations in some permutation. It therefore appears that there is no fundamental incon-

sistency between our determination of $[Fe/H]_{M71} = -1.27$ dex from four cluster members and the previous determinations. Reddening only affects our results indirectly, through T_{eff} determinations, with a maximum uncertainty of ± 100 K for an uncertainty in $E(B-V)$ of ± 0.06 mag, and its effects on the deduced abundances are, as shown in Table 4, small. Since the membership for our stars is certain and reddening does not significantly perturb our abundances, the values tabulated here are to be preferred over all previous determinations.

To further support our M71 results, we note that in the metal-rich open clusters NGC 2420 and M67, where the reddening is small and fairly well known, our results are consistent with those provided by $\delta(U-B)$. For NGC 2420, McClure, Forrester, and Gibson (1974) found [Fe/H] (NGC 2420 − Hyades) = −0.5 dex, while we find $[Fe/H]_{NGC\,2420} = -0.61$. Eggen and Sandage (1964) found M67 to be slightly metal poor compared to the Hyades, and we obtain [Fe/H] = −0.39. Griffin (1975, 1979) has performed a curve-of-growth analysis for two members of M67, and for the least uncertain elements (Ti, Cr, Fe, Ni), the difference between the average of her two stars and my four stars is in all cases less than 0.05 dex.

We thus find our abundances for M67 and NGC 2420 to be in good agreement with previous determinations and can invoke reasonable explanations (reddening and field-star contamination) for the difference between our results for M71 and all previous studies.

b) Implication of the M71 Abundance

The abundance we have obtained for M71 is considerably below previous estimates. It also appears from the work of Pilachowski, Canterna, and Wallerstein (1980) that the abundance of 47 Tuc has been overestimated in the past; they derive $[Fe/H]_{47\,Tuc} = -1.2$ dex, very close to our result $[Fe/H]_{M71} = -1.27$ dex. An analysis of Stromgren photometry of 47 Tuc red horizontal-branch stars by Dickens, Bell, and Gustafsson (1979) provides additional evidence for a somewhat lower abundance for this cluster. The first implication of these new determinations is that the correlation found by Carney (1980) between the metallicity of globulars and their age disappears. With half-solar metallicity, Carney found ages less than 10 billion yr for M71 and 47 Tuc, considerably younger than those of the metal-poor globulars. However, using the new lower metallicities makes the ages of 47 Tuc and M71 much older, comparable to those of other globulars. Furthermore, the problems described by Demarque and McClure (1977*a*) in the appearance of the color-magnitude diagram of 47 Tuc relative to that of NGC 2420 disappear as a result of the new metallicities. These determinations also affect the studies of synthesis of colors and spectral features in galaxies by Mould (1978), Cohen (1979*c*), and Aaronson *et al.* (1978). All of these authors explicitly assumed $[Fe/H]_{47\,Tuc} = -0.3$ and used the observed 47 Tuc color-magnitude diagram to remove the effects of uncertainties in the treatment of convection in the stellar evolutionary computations and resulting bolometric luminosity functions of Ciardullo and Demarque (1977). Therefore there may be a large scale error in the results of these programs such that galaxy abundances are overestimated; the size of this error is currently being evaluated.

Substantially lower abundances than previously accepted have been deduced for M71 here and for 47 Tuc by Pilachowski, Canterna, and Wallerstein (1980); there is every reason to expect that this phenomenon is not confined to these particular two clusters, and that the entire scale of abundances for the "metal rich" globulars is incorrect in the sense of being too metal rich. Although this conjecture is somewhat spectulative, its consequences are important and in many ways simplify the picture of the chemical history of the Galaxy. There may well be a gap, or at least only a very moderate region of overlap, between the abundance range over which the globular clusters are found and that over which open clusters occur. The older scenario required many globulars which are far older than M67 or NGC 2420 to be more metal rich than NGC 2420. In the emerging new picture, this gap in abundance corresponds well to the gap in age, estimated to be at least 10×10^9 yr for globulars and about 5×10^9 yr for the oldest known open clusters (Demarque and McClure 1977*b*). We thus support the picture of the formation of the halo stars (i.e., the globular clusters) occurring within a small time span but with widely varying metallicities. The disk then formed later, but even initially had a metallicity equal to that of the most metal-rich globular.

In this context, the questions of how much mass was lost from globular clusters in the course of their formation and what fraction of the original population of globular clusters failed to survive to the present epoch (see, for example, Lightman, Press, and Odenwald 1978) assume greater importance. It is also no longer clear that variation of metallicity alone within the smaller abundance range now proposed is adequate to produce the full range of horizontal branch (HB) distributions from exclusively red HB stars to exclusively blue HB stars seen in globular clusters. Much theoretical work will be required to clarify these issues.

Although our results do not affect the relative ranking of globular clusters within the many classifications and ordering schemes used, such as those of Searle and Zinn (1978) and of Zinn (1980), the scale at the upper end is altered. In particular, the linear relationship between Q39 and [Fe/H] used by Zinn (1980) probably becomes highly nonlinear at $[Fe/H]_{Zinn} \geq -1.3$. Much future work will be necessary to verify that indeed the whole scale of metal-rich clusters is too over abundant (i.e., that M71 and 47 Tuc are not anomalous in this regard) and to provide enough valid metallicity determinations so that photometric systems can be correctly calibrated.

V. SUMMARY

High-dispersion echelle spectra of four giants in the metal-rich globular cluster M71, of four stars in the old open cluster M67, and of two members of NGC 2420 are analyzed with the aid of model atmospheres. The most

important result is that in strong contrast to older determinations the globular cluster M71 is found to have a metallicity [Fe/H] = −1.27 dex with respect to the Sun, while the old open clusters M67 and NGC 2420 have [Fe/H] = −0.39 and −0.61 dex, respectively, similar to values obtained by previous investigators. The problems of large, uncertain reddening and possible strong contamination by field stars appear to have led to erroneously high abundances being deduced in the past for M71. A suggestion is made that the entire metal-rich end of the globular cluster abundance range has been systematically overestimated by previous investigators, and that there is no, or at most a very small, region of overlap between the abundance range occupied by galactic globular clusters and that of old open clusters. This gap in abundance fits in well with the gap in age between the youngest globular and the oldest open cluster. Thus it is suggested that the halo formed over a wide range in metallicity from roughly $\frac{1}{200}$ to $\frac{1}{10}$ the solar value, while the disk of the Galaxy formed later from material at least as enchanced in metals as the most metal-rich globular cluster.

The pattern of abundance distribution of elements with respect to Fe is examined in M92, M13, M17, NGC 2420, and M67. The similarity of the distributions, especially for the best-determined elements from Ca to Fe, over this range of approximately a factor of 100 in Fe/H is amazing. Ignoring factors of 2, nucleosynthesis and dispersion of processed material of these elements proceeded identically over large regions of space, time, and metallicity. Some subtle differences in the abundance distribution are noted. Probably real is the decrease in Cu/Fe as metallicity decreases; possibly real trends include larger Ca/Fe and smaller rare earths/Fe as metallicity decreases. O/Fe appears to follow Ca/Fe and hence may be larger in the globulars than in the more metal-rich open clusters.

There is no detectable spread in the abundance of the heavy elements within the three clusters studied here.

APPENDIX

We present in Table 8 some data on the radical velocities, interstellar lines, and Hα profiles of the program stars in M71, M67, and NGC 2420. None of the giants studied in these clusters showed believable evidence for emission in the wings of H_α. The heliocentric radial velocities are given in the second column, and agree well with the determinations by Jenner and Kwitter (1977) for M71 and by Popper (1954) for M67; however the mean V_r obtained by McClure, Forrester, and Gibson (1974) from three stars in NGC 2420 is 110 km s^{-1}, in substantial disagreement with our value measured from considerably higher-dispersion spectra.

The M71 stars showed a strong interstellar component, so blended with the stellar Na D lines that no separation was possible, with a heliocentric radial velocity close to 0 km s^{-1}. A much weaker, but still detectable interstellar component was seen in all the M67 stars at a velocity close to −13 km s^{-1}. Because of the strong stellar lines, it was impossible to obtain a reliable doublet ratio, and hence only a crude estimate of the Na column density and expected reddening is available. With an uncertainty of a factor of 2, the Na I column density in front of M67 is 2×10^{12} atoms cm^{-2}, implying

TABLE 8

V_r AND INTERSTELLAR Na COMPONENTS

		Interstellar Na						
		Component 1			Component 2			Stellar
Star	V_r (km s^{-1})	W_λ(5889) (mÅ)	W_λ(5895) (mÅ)	V_r (km s^{-1})	W_λ(5889) (mÅ)	W_λ(5895) (mÅ)	V_r (km s^{-1})	Hα (W_λ[Å])
M71:								
A4	−28	...	...	[a]	...	...	...	1.11
30	−26	...	...	[a]	...	...	...	1.03
45	−22	...	...	[a]	...	...	...	1.07
46	−26	...	...	[a]	...	...	...	1.06
M67:								
105	+32	142:	113:	−14	...	...	...	1.06
170	+32	[b]	[b]	−12	...	...	...	1.13
224	+29	[b]	[b]	−13	...	...	...	1.16
231	+32	[b]	[b]	−13	...	...	...	1.03
NGC 2420:								
A	+76	240:	196:	+11	[c]	[c]	−17	1.15
F	+74	196:	152:	+18	[c]	[c]	−12	1.19

[a] Very strong interstellar component, $V_r \approx 0$ km s^{-1}, present in all M71 stars.
[b] Line too blended with stellar Na I to measure W_λ.
[c] Weak, but both components definitely present.

$E(B - V) = 0.09$ mag using the methods and constants of Paper I. This result is too uncertain to aid in choosing between the estimates of $E(B - V)$ ranging from 0.03 to 0.10 mag advocated by various previous photometric investigations of M67.

The NGC 2420 stars show two interstellar components. The stronger of them corresponds approximately to a reddening of 0.14 mag, which can only be forced as low as to $E(B - V) = 0.05$ mag by assuming that the doublet ratio, determined from the somewhat uncertain measured equivalent widths of the interstellar component to be 1.25, is actually 2.0. Thus the strong interstellar lines we observe suggest that the low reddening of $E(B - V) = 0.02$ mag for NGC 2420 found by McClure, Forrester, and Gibson (1974) and used here is actually larger.

REFERENCES

Aaronson, M., Cohen, J. G., Mould, J. R., and Malkan, M. 1978, *Ap. J.*, **223**, 824.
Arnett, W. D. 1971, *Ap. J.*, **166**, 153.
Arp, H. C., and Hartwick, F. D. A. 1971, *Ap. J.*, **167**, 499.
Biehl, D. 1976, Ph.D. thesis, Kiel University.
Butler, D. 1975, *Ap. J.*, **200**, 68.
Canterna, R. 1975, *Ap. J.* (*Letters*), **200**, L63.
Carney, B. W. 1980, *Ap. J.*, **236**, 318.
Ciardullo, R., and Demarque, P. 1977, *Trans. Astr. Obs.*, Vol. **35**.
Cohen, J. G. 1978, *Ap. J.*, 487 (Paper I).
———. 1979*a*, *Ap. J.*, **231**, 751 (Paper II).
———. 1979*b*, in *IAU Symposium 85*, *Starclusters* (Dordrecht: Reidel, in press).
———. 1979*c*, *Ap. J.*, **228**, 405.
Cohen, J. G., Frogel, J. A., and Persson, S. E. 1978, *Ap. J.*, **222**, 165 (CFP).
Corliss, C. H., and Bozman, W. R. 1962, in *Experimental Transition Probabilities for Spectral Lines of Seventy Elements*, NBS Monog. No. 53.
Demarque, P., and McClure, R. D. 1977*a*, *Ap. J.*, **213**, 716.
———. 1977*b*, in *The Evolution of Galaxies and Stellar Populations*, ed. B. M. Tinsley and R. B. Larson (New Haven: Yale University Press).
Dickens, R. J., Bell, R. A., and Gustafsson, B. 1979, *Ap. J.*, **232**, 428.
Eggen, O. J., and Sandage, A. R. 1964, *Ap. J.*, **140**, 130.
Frogel, J. A., Persson, S. E., and Cohen, J. G. 1979, *Ap. J.*, **227**, 499.
Griffin, R. 1975, *M.N.R.A.S.*, **171**, 181.
———. 1979, *M.N.R.A.S.*, **187**, 277.
Gustafsson, B., Bell, R. A., Eriksson, K., and Nordland, A. 1975, *Astr. Ap.*, **42**, 407.
Hartwick, F. D. A., and Hesser, J. E. 1974, *Ap. J.* (*Letters*), **194**, L129.
Hesser, J. E., Hartwick, F. D. A., and McClure, R. D. 1977, *Ap. J. Suppl.*, **33**, 471.
Jenner, D. C., and Kwitter, K. B. 1977, *Bull. AAS*, **9**, 287.
Kurucz, R. L. 1979, *Ap. J. Suppl.*, **40**, 1.
Lightman, A. P., Press, W. H., and Odenwald, S. F. 1978, *Ap. J.*, **219**, 629.
McClure, R. D., Forrester, W. T., and Gibson, J. 1974, *Ap. J.*, **189**, 409.
Mould, J. R. 1978, *Ap. J.*, **220**, 434.
Mould, J. R., and McElroy, D. 1978, *Ap. J.*, **221**, 580.
Murray, C. A., Corben, P. M., and Allchorn, M. R. 1965, *Royal Obs. Bull.*, No. 91.
Pilachowski, C. A., Canterna, R., and Wallerstein, G. 1980, *Ap. J.* (*Letters*), **235**, L21.
Popper, D. M. 1954, *A.J.*, **59**, 445.
Ridgway, S. T., Joyce, R. R., White, N. M., and Wing, R. F. 1980, *Ap. J.*, **235**, 126.
Searle, L., and Zinn, R. 1978, *Ap. J.*, **225**, 357.
Tifft, W. G. 1963, *M.N.R.A.S.*, **126**, 209.
Zinn, R. 1980, *Ap. J. Suppl.*, **42**, 19.

JUDITH G. COHEN: 105-24, California Institute of Technology, Pasadena, CA 91125